

# Methodical aspects in the surface analysis of supported molybdena catalysts

Laura E. Briand,<sup>1</sup> Olga P. Tkachenko,<sup>2,5</sup> Monica Guraya,<sup>3,5</sup> Israel E. Wachs<sup>4</sup> and Wolfgang Grünert<sup>5\*</sup>

<sup>1</sup> Centro de Investigación y Desarrollo en Ciencias Aplicadas, Dr. Jorge J. Ronco-Universidad Nacional de La Plata, Consejo Nacional de Investigaciones Científicas y Técnicas, Calle 47 No 257, C.C. 59, (B1900AJK) La Plata, Buenos Aires, Argentina

<sup>2</sup> Permanent address N. D. Zelinsky Institute of Organic Chemistry, Russian Academy of Sciences, Moscow, Russia

<sup>3</sup> Permanent address Centro Atomico Bariloche, CNEA, Argentina

<sup>4</sup> Operando Molecular Spectroscopy and Catalysis Laboratory, Department of Chemical Engineering, Lehigh University, Bethlehem, PA 18015, USA

<sup>5</sup> Lehrstuhl für Technische Chemie, Ruhr-Universität Bochum, D-44780 Bochum, Germany

Received 25 September 2003; Revised 5 December 2003; Accepted 5 December 2003

Supported molybdena catalysts, with TiO<sub>2</sub>, CeO<sub>2</sub> and Al<sub>2</sub>O<sub>3</sub> supports, were studied by XPS and ISS. It was found that reliable results are obtained only when samples are calcined and transferred into the ultrahigh vacuum system without further contact with the ambient atmosphere ('*in situ* calcination'). This applies also to catalysts that were previously calcined but had been stored in the ambient atmosphere. Supported Mo oxide becomes reduced under x-ray irradiation during extended XPS data acquisition. A slight decrease of the Mo/support cation intensity ratio as a consequence of this reduction was detected by ISS in MoO<sub>3</sub>/TiO<sub>2</sub> and MoO<sub>3</sub>/CeO<sub>2</sub>, therefore ISS analysis should be performed on freshly calcined samples without prior extended exposure to x-rays. Because ISS spectra change rapidly due to sputtering, a correct analysis of the surface properties of the supported Mo catalyst requires extrapolation of the trend to the start of the experiment. It was established by this methodology that the surface of a 7% MoO<sub>3</sub>/TiO<sub>2</sub> catalyst (5.3 Mo nm<sup>-2</sup>) is completely covered by a monolayer of Mo oxide species, and no Ti cation is exposed. In a submonolayer MoO<sub>3</sub>/CeO<sub>2</sub> catalyst the exposed support could be detected, as expected, whereas in an MoO<sub>3</sub>/Al<sub>2</sub>O<sub>3</sub> catalyst with an Mo oxide loading equal to the monolayer coverage a slight exposure of the Al support cation also was noted probably because of the high curvature of the smaller Al<sub>2</sub>O<sub>3</sub> particles. Copyright © 2004 John Wiley & Sons, Ltd.

**KEYWORDS:** molybdena; supported catalysts; ISS; XPS

## INTRODUCTION

In supported transition-metal oxide catalysts the interaction between the supported oxides (e.g. Mo(VI), V(V), W(VI)) and the oxide support (typically Al<sub>2</sub>O<sub>3</sub>, TiO<sub>2</sub>, ZrO<sub>2</sub>, excluding SiO<sub>2</sub>) is so strong that the formation of bulk transition-metal oxide species is observed only at high transition metal content. It is, however, still a matter of debate if aggregation of the transition metal oxide phase starts already while parts of the oxide support are still bare or if the support surface is first covered by a dense monolayer of surface transition-metal (Mo, V, W, etc.) oxide species before the transition-metal oxide starts to grow into the third dimension. The latter view is suggested by a number of studies mainly with vibrational spectroscopies, which are summarized in Refs 1–3. However, this view is now not supported by surface

analytical work, although supported Mo oxide catalysts are investigated by surface analytical techniques, particularly XPS, quite frequently.

X-ray photoelectron spectroscopy has been used both to determine surface concentrations of Mo oxide species on supports and oxidation states of Mo in reduced catalysts. Much of the early work is summarized in Refs 4–6. Some alternative approaches, in particular the use of the Auger parameter (chemical state plots) and of oxygen Auger signals, are stressed in Ref. 7. In the study of reduced Mo oxide catalysts the assignment of binding energies to Mo oxidation states has been a matter of controversy since the pioneering work of Cimino<sup>8</sup> and Haber<sup>9</sup> (see Refs 10–13). Only in rare cases can XPS differentiate species of an element that are in identical oxidation states. The use of XPS with fully oxidized supported metal oxide catalysts is therefore normally limited to comparisons between the surface and bulk metal/support-ratios. They tend to be proportional to each other below the theoretical monolayer coverage, whereas the surface ratio levels off or changes to a smaller increase above this limit. However, XPS is not suitable for deciding if the support was completely covered before a second monolayer

\*Correspondence to: Wolfgang Grünert, Lehrstuhl für Technische Chemie, Ruhr-Universität Bochum, PO Box 102148, D-44780 Bochum, Germany. E-mail: w.gruenert@techem.rub.de  
Contract/grant sponsor: USA National Science Foundation;  
Contract/grant number: CTS-9901643.  
Contract/grant sponsor: CONICET.

was formed. Owing to its average sampling depth of 1.5–2.5 nm (only ~30% of the signal intensity arises from the outermost sample layer) and the considerable errors inherent in intensity evaluation, a significant part of the supported oxide species could be deposited onto the first layer instead of the bare oxide support before the XPS line intensities are affected significantly. For flat samples, angular-dependent XPS analysis can improve the surface sensitivity, but its perspective is much less favourable with the curved surfaces of real catalyst powders.

Owing to its sensitivity exclusively to the outermost surface layer, ISS is better suited to study the problem if an oxide support carrying transition-metal oxide species in a quantity corresponding to the theoretical monolayer limit is completely covered by the supported oxide. Ion scattering spectroscopy has been applied frequently to supported oxide catalysts<sup>10,14–19</sup>, and several of these studies have resulted in the conclusion that aggregation of the transition-metal oxide species occurs before the monolayer coverage is completed.<sup>16–19</sup> In combination with chemisorption techniques, ISS even has been employed to determine surface coverages quantitatively.<sup>10,16,20</sup> The method is based on quantitative use of the Al/O ISS intensity ratios, which decrease with increasing transition-metal oxide content. On the basis of such measurements it has been argued that the support is only covered to ~85% (55%) in  $\text{WO}_3/\text{TiO}_2$  ( $\text{WO}_3/\text{ZrO}_2$ ) catalysts with tungsten contents above the theoretical monolayer surface coverage.<sup>18,21</sup> Formation of transition-metal oxide multilayers at incomplete coverage of the oxide support has been claimed also for  $\text{V}_2\text{O}_5/\text{Al}_2\text{O}_3$  catalysts,<sup>16</sup> and in early studies of alumina-supported Mo and W oxides the support line was still detected at transition-metal oxide contents far above the theoretical monolayer surface coverage.<sup>10,15</sup>

The history of the samples studied is not always clear in the literature. Although a calcination of the samples is usually mentioned it is not obvious if the calcined samples have been exposed to the ambient atmosphere prior to the surface spectroscopic investigation or not. The aim of the present study is to re-evaluate the methodology of surface analytical studies with supported transition-metal oxide catalysts on the basis of recent insight into the surface chemistry of these systems. It has been reported that the adsorption of water leads to the aggregation of the surface transition-metal oxide species into structures such as  $\text{V}_{10}\text{O}_{28} \cdot \text{H}_2\text{O}$  or  $\text{Mo}_7\text{O}_{24} \cdot \text{H}_2\text{O}$ ,<sup>2,3</sup> therefore any contact of the samples with the humidity-containing ambient atmosphere after calcination may obscure the results. In addition, if XPS analysis precedes the ISS study, the transition-metal oxide surface species may become reduced under the x-ray irradiation, depending on the measurement conditions. Such photoreduction during XPS has been described for supported vanadia catalysts.<sup>22,23</sup> It has been reported in the literature that transition-metal oxide surface species aggregate upon reduction in hydrogen.<sup>22,24–26</sup> Although this refers to thermal reduction at elevated temperatures, which favour the mobility of species, it cannot be excluded *a priori* that reduction of the transition-metal oxide species during x-ray exposure leads to a similar effect. Finally, it is well known that ISS is a destructive technique and that the

spectra of supported oxide catalysts will change gradually as the supported oxide is peeled off the oxide support. Extrapolation of the experimental data to the beginning of the experiment may be necessary, therefore, to derive reliable evidence about the sample studied.

In our study, the influence of these processes (*in situ* calcination, photoreduction, sample damage during ISS) on the result of ISS studies with supported oxides has been investigated and a new methodology has been derived. The present paper exemplifies this methodology with supported molybdena catalysts. The study of a series of supported vanadia catalysts will be published elsewhere.<sup>27</sup>

## EXPERIMENTAL

### Materials

The supported molybdena catalysts used for the present studies were prepared by the incipient-wetness impregnation method with aqueous solutions of ammonium heptamolybdate ( $(\text{NH}_4)_6\text{Mo}_7\text{O}_{24} \cdot 4 \text{H}_2\text{O}$ ). The supports used were  $\text{TiO}_2$  (Degussa P-25,  $45 \text{ m}^2 \text{ g}^{-1}$ ),  $\text{Al}_2\text{O}_3$  (Harshaw,  $222 \text{ m}^2 \text{ g}^{-1}$ ) and  $\text{CeO}_2$  (Engelhard,  $36 \text{ m}^2 \text{ g}^{-1}$ ). After impregnation, the samples were dried overnight at 293 K and finally calcined at 723 K ( $\text{TiO}_2$ - and  $\text{CeO}_2$ -supported samples) or 773 K ( $\text{Al}_2\text{O}_3$ -supported samples). The molybdena content (by inductively coupled plasma), surface Mo density and sample codes of the materials studied are summarized in Table 1. The surface Mo density at monolayer coverage is  $4.6 \text{ Mo atoms nm}^{-2}$  for  $\text{Al}_2\text{O}_3$ ,  $\text{TiO}_2$  and  $\text{CeO}_2$ .<sup>28</sup>

### Methods

The XPS and ISS spectra were measured with a Leybold surface spectrometer equipped with x-ray and ion sources and an EA 10/100 electron (ion) analyser with multi-channel detection (Specs). The samples (calcined materials after storage in contact with an ambient atmosphere) were deposited on the sample-holder from a slurry in *n*-pentane and introduced into the vacuum system without further pretreatment. This state will be referred to as 'stored in air'. Alternatively, these catalysts were re-calcined in flowing synthetic air (20%  $\text{O}_2/\text{N}_2$ ) at 730 K for 1 h in a pretreatment chamber of the surface spectrometer (i.e. on the sample-holder) before being introduced into the spectrometer vacuum without further contact with the ambient atmosphere.

The XPS spectra were recorded using  $\text{Mg K}\alpha$  excitation (1253.6 eV, 10 kV/20 mA), with the analyser in pass-energy

**Table 1.** Supported Mo oxide catalysts studied

Sample code	Actual composition	Surface Mo density (atoms $\text{nm}^{-2}$ )
5-Mo-Ti	5.5 wt.% $\text{MoO}_3/\text{TiO}_2$	3.8
7-Mo-Ti	7.5 wt.% $\text{MoO}_3/\text{TiO}_2$	5.3
10-Mo-Al	11.5 wt.% $\text{MoO}_3/\text{Al}_2\text{O}_3$	2.7
20-Mo-Al	24.5 wt.% $\text{MoO}_3/\text{Al}_2\text{O}_3$	5.6
3.5-Mo-Ce	2.7 wt.% $\text{MoO}_3/\text{CeO}_2$	3.6

mode (pass energy 35.5 eV). A sequential protocol was employed for data acquisition, with a sweep schedule covering the selected regions (Mo 3d, O 1s, the major support line and C 1s) being repeated many times. Because all intermediate results are saved in this protocol, the sample state can be inspected at any time. If beam damage is detected, the data that are to be summed for improvement of measurement statistics can be selected properly. Binding energies (BEs) were primarily referenced to C 1s = 284.5 eV, but the data given in Table 2 are related to the BE of the support cations as secondary references: Al 2p = 74.0 eV, Ti 2p<sub>3/2</sub> = 458.7 eV and Ce 3d<sub>5/2</sub> = 882.6 eV. The shifts between the calibrations relative to C 1s and to the support lines were minor for the TiO<sub>2</sub> and Al<sub>2</sub>O<sub>3</sub> supports. With CeO<sub>2</sub>, the C 1s BE could not be determined unambiguously because this region is superimposed by secondary Ce signals. Atomic ratios were calculated from intensity ratios by using Scofield interaction cross-sections<sup>29</sup> together with an empirical response function of the spectrometer sensitivity to the photoelectron kinetic energy.

The ISS spectra were measured with 2000 eV He<sup>+</sup> ions and the analyser in pass-energy mode (pass energy 195 eV). To record the changes of the sample surface caused by the measurement, sputter series were performed by defining narrow scans over the lines of interest (Mo, support cation). The excitation current was set at a low level to obtain spectra with still tolerable noise level at a minimized sputter rate. The surface charge was removed with a flood gun. After stabilization of source and flood gun with the sample withdrawn from the measurement position, the sample was moved into the He ion beam and the first scan was started

within 5 s. The length of the scans was typically 60–70 s, with the Mo signal appearing after ~50 s. From estimates of the sample current produced by the source employed, we believe that each scan takes away 5–10% of a monolayer. Scans including the oxygen signal were performed only at the end of the sputter series, which is, however, of limited value because the surface was then already far from the original state. Signal areas were integrated by assuming the background to be linear. Only in the case of MoO<sub>3</sub>/CeO<sub>2</sub>, where the Mo and Ce signals are not separated, was a curved background (analogous to the Shirley background in XPS<sup>30</sup>) employed (see Fig. 5).

## RESULTS

Typical Mo 3d spectra are shown in Fig. 1, and the signal shapes at the start and the end of overnight data acquisition periods that had been scheduled initially to obtain high-quality spectra are compared. It can be seen that the Mo 3d signal shape changes significantly, which indicates a reduction of Mo(VI) during data acquisition. The analysis of coexisting oxidation states in the Mo 3d spectra of oxide samples has long been a matter of controversy. The relation between binding energies and oxidation states preferred by most groups until recently assumes binding energy differences of 1.6 eV between Mo(VI) and Mo(V) and also between Mo(V) and Mo(IV).<sup>8,10,31</sup> Binding energy differences of 0.8 eV between these states have been assumed by some other groups.<sup>9,13</sup> Because the spectra presented in Fig. 1 reflect a very mild reduction, leading possibly to only one reduction product, they have been analysed by two different

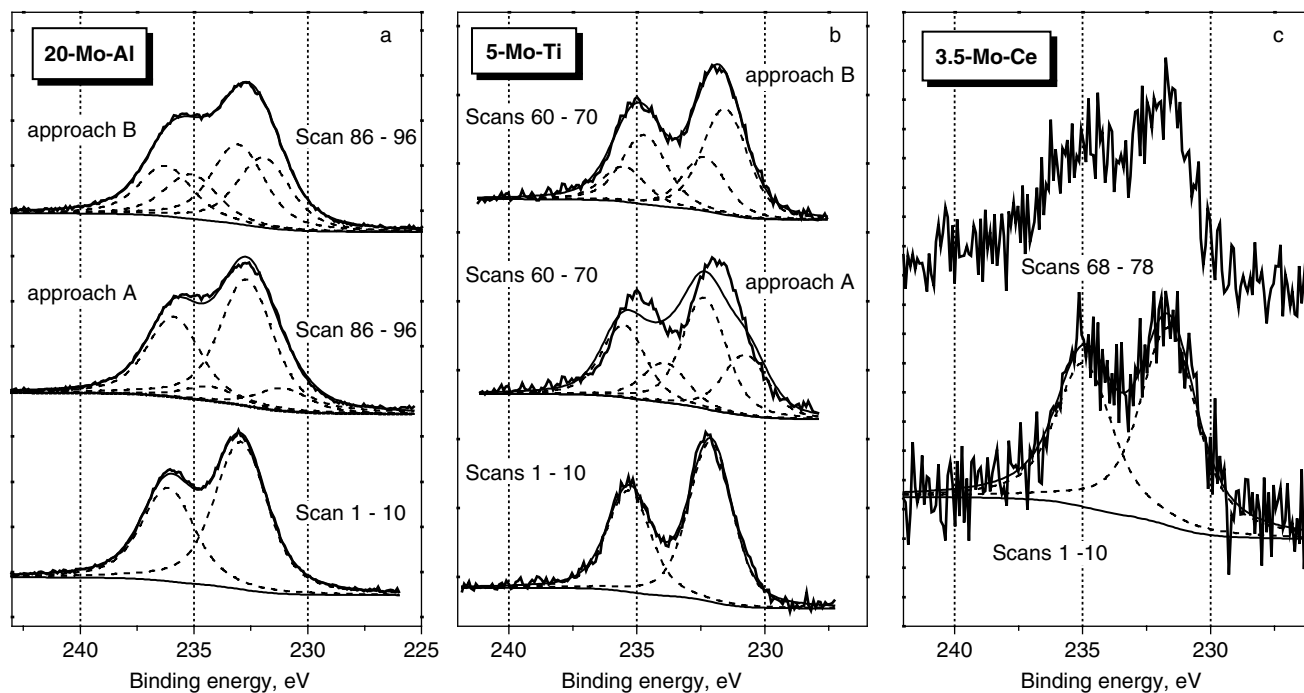


**Figure 1.** Evolution of Mo 3d XPS spectra of supported Mo oxide catalysts with data acquisition time and analysis of the changes with different approaches: approach A – binding energy difference between Mo(VI) and the second Mo state fixed at 1.6 eV (see text); approach B – binding energy fitted without constraint. (a) MoO<sub>3</sub>/Al<sub>2</sub>O<sub>3</sub> (20-Mo-Al); fit result: Mo(VI) at 232.5<sub>5</sub> eV (52%), second Mo state at 231.4 eV (48%). (b) MoO<sub>3</sub>/TiO<sub>2</sub> (5-Mo-Ti); fit result: Mo(VI) at 232.4<sub>5</sub> eV (32%), second Mo state at 231.2<sub>5</sub> eV (68%). (c) MoO<sub>3</sub>/CeO<sub>2</sub> (3.5-Mo-Ce). All samples studied after *in situ* calcination at 730 K.

**Table 2.** The XPS binding energies and surface atomic ratios measured with supported Mo catalysts

Sample	Treatment	Binding energy (eV)		Atomic ratio	
		Mo 3d <sub>5/2</sub>	O 1s	Mo/support <sup>a</sup>	support <sup>a</sup> /O
10-Mo-Al	Stored in air <sup>b</sup>	232.7	531.0	0.062	0.61
	After <i>in situ</i> calcination <sup>c</sup>	232.8	530.9	0.070	0.63
20-Mo-Al	Stored in air <sup>b</sup>	232.5 <sub>5</sub>	531.0	0.093	0.61
	After <i>in situ</i> calcination <sup>c</sup>	232.4 <sub>5</sub>	531.0	0.12	0.64
7-Mo-Ti	After <i>in situ</i> calcination <sup>c</sup>	232.6	530.0	0.29	0.31
3.5-Mo-Ce	After <i>in situ</i> calcination <sup>c</sup>	231.8	529.5	0.25	0.50

<sup>a</sup> Al, Ti or Mo.

<sup>b</sup> Calcined at 723 K, but studied after prolonged contact with the humidity-containing ambient atmosphere.

<sup>c</sup> Calcination for 1 h at 730 K with 20% O<sub>2</sub> in N<sub>2</sub>.

approaches to gain further evidence for a decision about the relation between BEs and oxidation states. In both cases the line shapes were kept invariable: in method A the second Mo oxidation state was assumed to be at a 1.6 eV lower BE than Mo(VI), while its binding energy was varied in method B. It is clear from Fig. 1 that it is not possible to fit the spectra of samples 20-Mo-Al and 5-Mo-Ti with method A but method B yields a second Mo state at 1.1–1.2 eV below Mo(VI). In the case of 3.5-Mo-Ce, the large noise did not permit a differentiation between the results obtained with the two approaches.

In Table 2, binding energies and elemental ratios measured with supported molybdena catalysts are summarized. The binding energies are well within the range reported in the earlier literature.<sup>10–12</sup> The influence of the *in situ* calcination step on the spectra is exemplified with the alumina-supported catalysts. It can be seen that the Mo/Al atomic ratio increases upon re-calcination, which indicates a redispersion of Mo oxide species on the alumina during the thermal treatment.

An example of the ISS sputter series (sample 7-Mo-Ti) is given in Fig. 2. It can be seen how the Ti signal increases with ongoing sputtering while the Mo signal decreases, which results in a monotonous decrease of the Mo/Ti ratio. However, it is quite clear that the Ti signal is present even in the first scan of this sample, the surface Mo density of which exceeds that at monolayer surface coverage.

Ion scattering spectra (first scans) of Mo/Al<sub>2</sub>O<sub>3</sub> catalysts without and after *in situ* calcination in air are compared in Fig. 3. It is quite clear that the Mo/Al intensity ratio is significantly affected by the *in-situ* calcination. As in the case of XPS, the Mo/Al ratios increase but the effect is more pronounced in the more surface-sensitive ISS. Again, in the monolayer 20-Mo-Al catalyst, the Al signal is present already in the first scan.

The influence of a previous XPS measurement on the ISS spectra is demonstrated for sample 7-Mo-Ti in Fig. 4. The first five scans for a fresh sample and a sample after XPS analysis (both after *in situ* calcination) are given in Figs 4(a) and 4(b). Despite the larger experimental noise in the measurement without previous exposure to x-rays, it is quite apparent that the Ti signal is attenuated in this series. In the first scans it is hard to identify at all, but integration over the relevant kinetic energy range yields a non-zero value. The

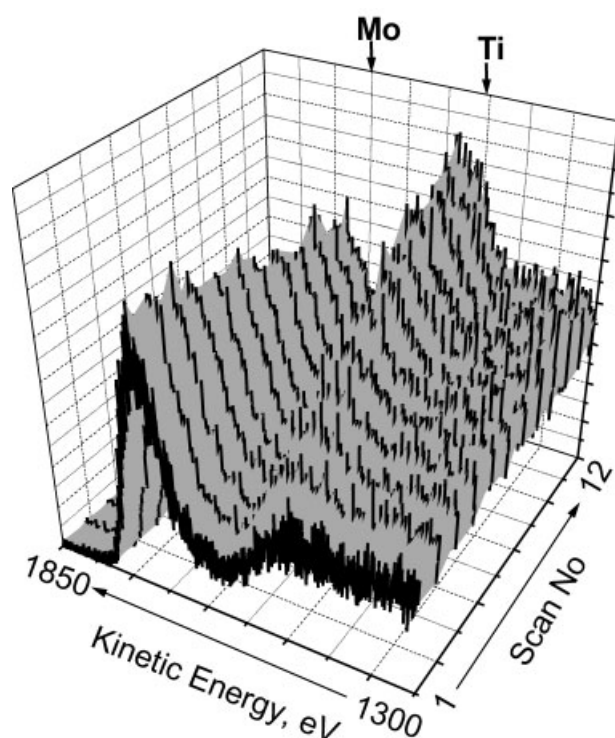


**Figure 2.** Example of ISS sputter series taken from a 7 wt.% MoO<sub>3</sub>TiO<sub>2</sub> catalyst (*in situ* calcined at 730 K, ISS spectra recorded after previous XPS analysis).

Ti/Mo area ratios are plotted versus the scan number in Fig. 4(c). Despite some scatter it is obvious that the Ti/Mo ratios are smaller with the sample not exposed previously to the x-ray beam, i.e. the Ti cations are less exposed in this case. Figure 4(c) presents also the linear fits over the first 10 scans for both samples. Only for the fresh sample does this linear fit go through the origin (i.e. the TiO<sub>2</sub> support was completely covered by surface Mo oxide species in the calcined 7-Mo-Ti sample). The fit parameters together with their confidence intervals are given in the legend to Fig. 4, and it is obvious that the confidence intervals of the intercept do not overlap for the series with and without extended exposure to x-rays. Therefore, the effect of the photoreduction on the surface Mo oxide coverage is significant.

Figure 5 gives similar information for sample 3.5-Mo-Ce. Figure 5(a) presents examples for the peak fitting required to

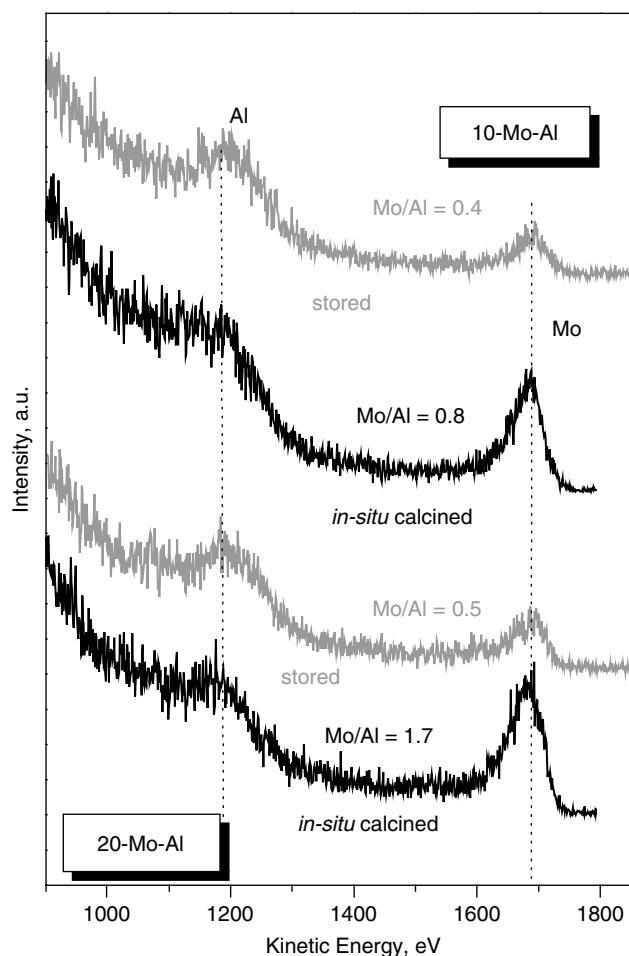


**Figure 3.** Influence of *in situ* calcination on the ISS spectra of  $\text{MoO}_3/\text{Al}_2\text{O}_3$  catalysts. 'Stored' samples are calcined at 723 K in air but are studied after prolonged contact with the humidity-containing ambient atmosphere; all ISS spectra are taken after previous XPS measurement.

extract the Ce and Mo signal areas from the superimposed signals. In the sputter series, the Ce/Mo ratio levelled off or even decreased slightly above the fifth scan, which is not yet well understood. Nevertheless, an extrapolation to describe the initial state of the samples is still possible with the first scans as shown in Fig. 5(b). It can be seen that exposure to x-rays has an effect on the ISS spectra also in this case: although the levelling off of the Ce/Mo ratios causes some uncertainties in the extrapolations, the ranges for the initial Ce/Mo values are different before and after x-ray exposure, with a smaller initial Ce/Mo ratio in the fresh sample. The extrapolation does not, however, go through the origin. It appears from this that the  $\text{CeO}_2$  support was not completely covered by surface Mo oxide species in the 3.5-Mo-Ce sample.

The results obtained with sample 20-Mo-Al are summarized in Fig. 6. In the spectra of alumina-supported catalysts, the Al signal appears on a background declining from the oxygen signal (cf. Fig. 3). This makes a correct integration of the Al signal difficult, although the presence even of weak signals can be qualitatively well identified. Figure 6 shows that the Al/Mo ratios level off after some time. A significant influence of the previous exposure to x-rays on the ISS

spectra cannot be detected in this system. Despite the considerable scatter due to the uncertainties in peak integration, it is clear that the Al/Mo ratios do not extrapolate to zero even although the initial Al/Mo intensity ratio is small.

## DISCUSSION

The present work demonstrates several influences that may affect the surface analysis of supported oxide catalysts, in particular by ISS. Figure 1 shows that supported Mo(VI) species may be reduced during extended XPS analysis, which to our knowledge has not been reported before in the literature. This is of relevance mainly for samples with low Mo content where long data acquisition may be required to obtain acceptable spectra, but it shows also that it is questionable to seek for quality improvement by long data accumulation in the analysis of higher loaded supported Mo oxide catalysts. The Mo  $3d_{5/2}$  binding energy of the reduction product is  $\sim 1.2$  eV lower than that of Mo(VI). Its assignment is not straightforward because it depends on the relation between Mo binding energies and oxidation states, which is still under debate for Mo oxide systems. A non-linear relation between Mo binding energies and oxidation states, which includes 1.6 eV shifts between Mo(V) and Mo(VI) and again between Mo(IV) and Mo(V),<sup>8,10,31</sup> later modified to 1.3 eV between Mo(VI) and Mo(V) but 1.9 eV between Mo(VI) and Mo(IV),<sup>11,12</sup> is widely accepted in the literature. However, there are groups that advocate a linear relation between Mo binding energy and oxidation state that involves 0.8 eV shifts of both Mo(V) to Mo(VI) and Mo(IV) to Mo(V) and assigns a state at 3.2 eV below Mo(VI) either to Mo(II) or to mutually bonded Mo(IV) ions.<sup>9,13</sup> In contrast to both approaches, Aigler *et al.* have demonstrated a Mo(VI)–Mo(IV) shift as small as 1.1 eV with photoreduced Mo/SiO<sub>2</sub> catalysts.<sup>32</sup> According to the latter, the reduction product formed during x-ray exposure of supported Mo catalysts would be Mo(IV), whereas it would have to be assigned as Mo(V) with the former approaches. Unfortunately, verification by independent techniques, e.g. oxygen consumption during reoxidation, is not possible with the samples studied here. The example illustrates the need for further research to establish a reliable binding energy scale for the assignment of Mo oxidation states.

Figure 2 demonstrates that the ISS spectra of supported oxide catalysts change rapidly due to the sputter effect of the He ions. With one exception cited above (3.5-Ce-Mo, *in situ* calcined, ISS after XPS, at higher scan numbers; not shown in Fig. 5), the general trend of the sputter series was always the same: from the first scan, the area ratio between the Mo (or V<sup>27</sup>) and the support ion decreases, which reflects uncovering of the support by peeling off the supported transition-metal oxide species. However, although the area ratio between the transition metal and the support cations went on to decrease to low values in many cases ( $\text{MoO}_3/\text{TiO}_2$ ,  $\text{V}_2\text{O}_5/\text{ZrO}_2$ ,  $\text{V}_2\text{O}_5/\text{CeO}_2$ ,  $\text{V}_2\text{O}_5/\text{Nb}_2\text{O}_5$ <sup>27</sup>), it tended to level off with  $\text{MoO}_3/\text{Al}_2\text{O}_3$  (and  $\text{V}_2\text{O}_5/\text{Al}_2\text{O}_3$ <sup>27</sup>). This can be understood by considering the difference in BET surface area between these supports. A complete removal of the supported transition-metal oxide species can be expected

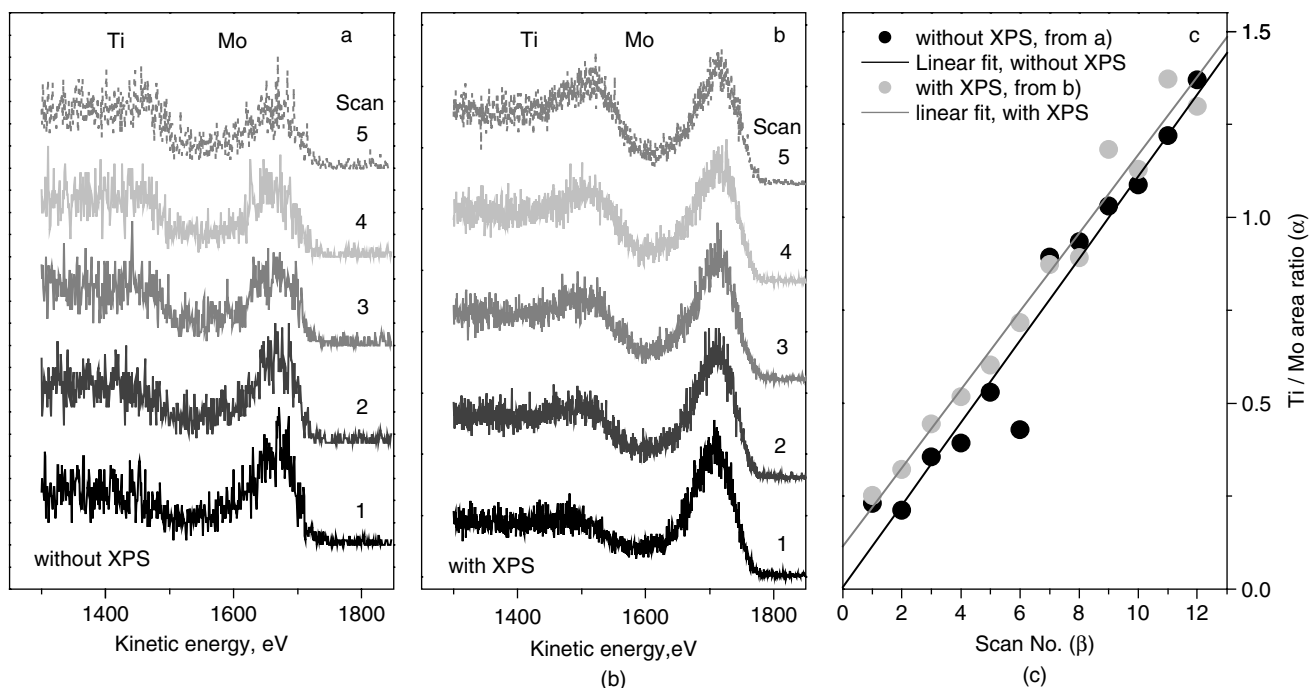


**Figure 4.** Influence of extended exposure to x-rays (XPS analysis) on the ISS spectra of 7-Mo-Ti: (a, b) first ISS scans in runs without (a) and with (b) previous XPS measurement, samples calcined *in situ* at 730 K; (c) evolution of the Ti/Mo intensity ratio ( $\alpha$ ) with ongoing analysis (scan number  $\beta$ ), together with linear fits of the data (fit curves, with confidence intervals, with XPS:  $\alpha = (0.116 \pm 0.039) + (0.105 \pm 0.005) \beta$ ; without XPS:  $\alpha = (0.006 \pm 0.058) + (0.110 \pm 0.008) \beta$ ).

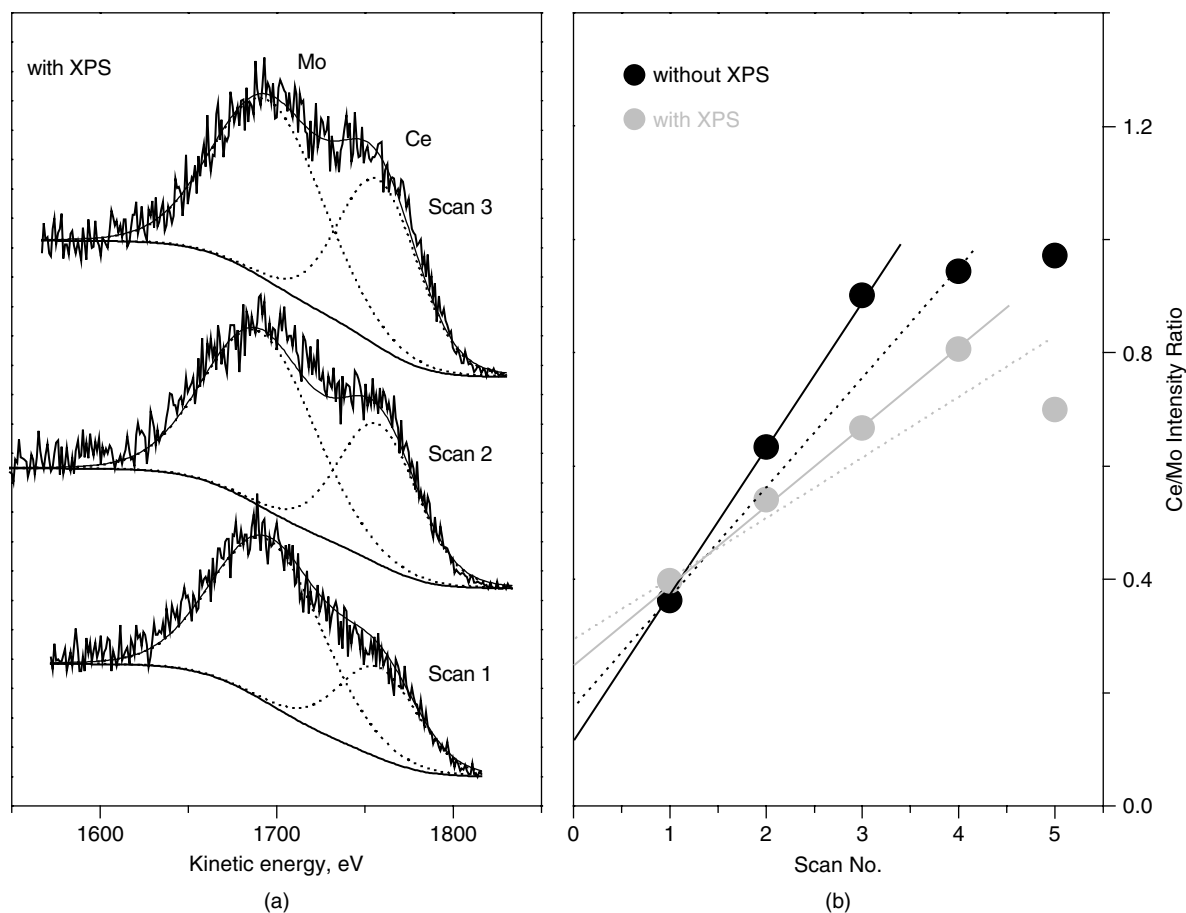


**Figure 5.** Influence of extended exposure to x-rays (XPS analysis) on the ISS spectra of 3.5-Mo-Ce: (a) examples for the mathematical separation of Mo and Ce signals (sample calcined *in situ* at 730 K; ISS spectra taken after previous XPS analysis); (b) evolution of the Ce/Mo intensity ratio in the first scans, together with extrapolations to scan zero.

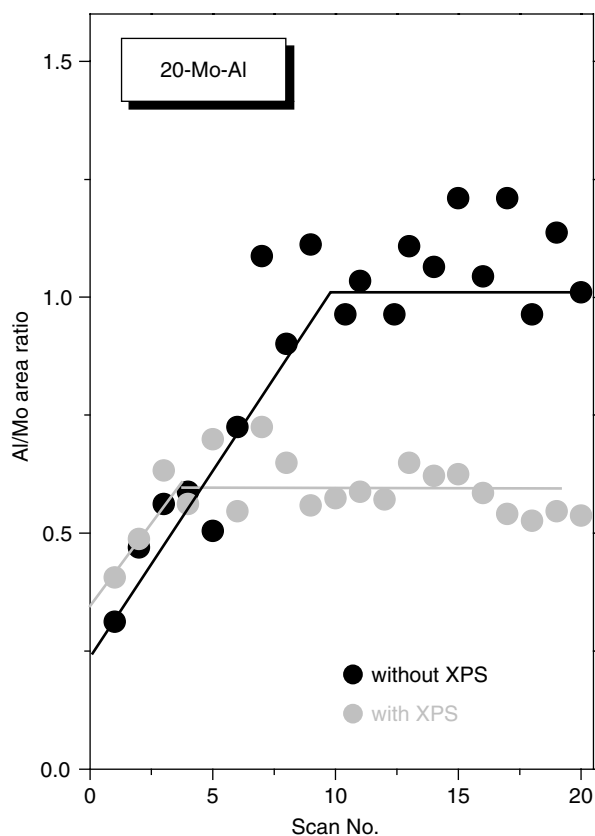


**Figure 6.** Evolution of the Al/Mo intensity ratio in ISS sputter series with 20-Mo-Al. Samples calcined *in situ* at 730 K.

only for a flat surface at right angles to the analyser direction, which is best approximated by low-area supports. A high surface area support such as  $\text{Al}_2\text{O}_3$  will present most surfaces at various angles to the analyser where the transition-metal oxide species and the support cations are peeled off simultaneously after a short initial period. The 3.5-Mo-Ce sample does not behave according to this model: although it has a low BET surface area, the Mo/Ce ratios level off after a short time (cf. Fig. 5). A possible explanation for this may be that the  $\text{CeO}_2$  used does not arise from a high-temperature preparation such as the  $\text{TiO}_2$  and  $\text{ZrO}_2$  supports employed. The latter should have more flat and regular facets than the former, which should have an irregular rough surface despite the rather low total surface area causing the sputter series to adopt a similar trend to that with  $\text{Al}_2\text{O}_3$ .

The rapid change of the ISS spectra invokes the necessity to perform sputter series with ion currents that are as low as possible. For traditional equipment this requires operation near the detection limits and will not usually produce high-quality spectra. Fortunately, the data treatment steps required (integration, extrapolation of trends) all tend to average out experimental noise. The extrapolation is favourably done with the support cation/transition-metal ion ratio, which extrapolates to zero for complete coverage of the support.

From Table 2 and Fig. 3 it is evident that a reliable analysis of the catalyst surface can be expected only when the sample was previously calcined and then transferred to the spectrometer without further contact with the ambient

atmosphere (*in situ* calcination). Again, this is confirmed by experience with supported vanadium oxide systems.<sup>27</sup> This observation supports the view that surface molybdenum oxide species become detached from the support surface under the influence of moisture and aggregate in the hydrated state (in the case of supported molybdena catalysis, for example, into  $\text{Mo}_7\text{O}_{24} \cdot (\text{H}_2\text{O})^{2,3}$ ). It might be argued that residual water (or carbon) may have attenuated the signals of the transition-metal cation in the non-calcined samples. However, measurable changes in the XPS intensity ratios can be expected only when the adsorbate layers on these samples are thick (if homogeneously distributed) or selectively deposited on the transition-metal ions. Both assumptions are in disagreement with the ISS results: the former would prevent the observation of any spectra; the latter would produce intermediate increases in the transition metal/support ion ratios, which was observed only in one case (with an *in situ* calcined sample, *vide supra*). Hence, the intensity changes observed upon *in situ* calcination (Table 1, Fig. 3) indicate a re-dispersion of the Mo oxide species on the surface. This agrees with conclusions from Raman- and infrared spectroscopic studies, according to which dehydration of the surface during calcination leads to decomposition of the Mo oxide clusters, and the Mo oxide species bind to the support and form a two-dimensional overlayer of isolated and oligomeric surface species.<sup>2,3</sup>

Although the essential role of the calcination process was expected on the basis of the recent literature, the changes in the ISS spectra after extended XPS analysis (which did not result in changes of the XPS intensity ratios) were surprising. The clustering of reduced transition-metal oxide species upon reduction has been reported for thermal reduction in  $\text{H}_2$ ,<sup>22,24–26</sup> where the conditions favour the mobility of species. Upon reduction under the x-ray beam, the clustering is, of course, less extensive but it was clearly detected in sample 7-Mo-Ti, with high probability also in sample 3.5-Mo-Ce. Other examples with supported vanadia catalysts may be found in Ref. 27. After taking this effect into account, it could be shown that the Ti cations are indeed completely covered by the surface Mo oxide monolayer (Fig. 4). This is a remarkable result despite the fact that the surface Mo density of this catalyst is somewhat above the monolayer limit, because it has been claimed sometimes in the literature that the support ( $\text{ZrO}_2$ ,  $\text{TiO}_2$ ,  $\text{Al}_2\text{O}_3$ ) remains exposed at transition metal oxide (W, Mo, V) loadings above monolayer surface coverage.<sup>16,18,21</sup> For  $\text{MoO}_3/\text{TiO}_2$  this is definitely not the case. Similar conclusions could be drawn for  $\text{V}_2\text{O}_5/\text{ZrO}_2$ ,  $\text{V}_2\text{O}_5/\text{CeO}_2$ , and  $\text{V}_2\text{O}_5/\text{Nb}_2\text{O}_5$  in Ref. 27.

For  $\text{MoO}_3/\text{CeO}_2$  and  $\text{MoO}_3/\text{Al}_2\text{O}_3$  catalysts, the support was found to be exposed to a small extent. In the case of  $\text{MoO}_3/\text{CeO}_2$ , this is according to expectations because the Mo surface density is below the monolayer limit in this sample (Table 1). On the other hand, with the  $\text{Al}_2\text{O}_3$  support a significant exposure of Al cations was found also in analogous  $\text{V}_2\text{O}_5/\text{Al}_2\text{O}_3$  catalysts<sup>27</sup> so that we consider this observation significant. We ascribe it tentatively to the stronger curvature of surfaces in the high-surface-area alumina support (primary particle diameters of  $d_p = 8 \text{ nm}$

and 35 nm estimated from the BET surface areas of the bare Al<sub>2</sub>O<sub>3</sub> and TiO<sub>2</sub> supports (cf. Experimental) with equation  $d_p = 6/(\rho A_{\text{BET}})$ , assuming spherical particles and density  $\rho = 3.4$  and  $3.9 \text{ g cm}^{-3}$  for  $\gamma$ -Al<sub>2</sub>O<sub>3</sub> and anatase, respectively), which may leave Al cations exposed even if the surface is saturated with Mo oxide (vanadium oxide) species.

## CONCLUSIONS

For surface analytical studies of supported transition-metal catalysts (here, supported Mo oxide catalysts) it is essential that the samples are calcined at a suitable temperature and studied without further contact with the atmosphere (*in situ* calcination). Storage of calcined catalysts at the ambient atmosphere results in significant decreases of the Mo/support ion signal intensity ratios in XPS and ISS. Supported Mo(VI) oxide species are reduced during extended XPS data acquisition. For MoO<sub>3</sub>/TiO<sub>2</sub> and MoO<sub>3</sub>/CeO<sub>2</sub> this reduction decreases the surface Mo oxide coverage slightly, as detected by ISS. Owing to the rapid change of the ISS spectra, the original state of the surface has to be derived by extrapolation of sputter series. In calcined MoO<sub>3</sub>/TiO<sub>2</sub> catalysts, the titania support was found to be completely covered by a close-packed monolayer of surface Mo oxide species when the Mo loading exceeds the monolayer surface coverage. In MoO<sub>3</sub>/Al<sub>2</sub>O<sub>3</sub>, a small part of the Al cations was still exposed at monolayer surface Mo oxide coverage probably due to the curvature of the smaller Al<sub>2</sub>O<sub>3</sub> particles.

## Acknowledgements

L.E.B. and I.E.W. gratefully acknowledge the financial support provided by the USA National Science Foundation (NSF), grant CTS-9901643, as well as the USA–Argentina International Collaboration grant between NSF (USA) and CONICET (Argentina).

## REFERENCES

1. Wachs IE. *Catal. Today* 1996; **27**: 437.
2. Deo G, Wachs IE, Haber J. *Crit. Rev. Surf. Chem.* 1994; **4**: 141.
3. Banares MA, Wachs IE. *J. Raman Spectrosc.* 2002; **33**: 359.
4. Barr T. In *Practical Surface Analysis* (2nd edn), vol. 1, Briggs D, Seah MP (eds). John Wiley: Chichester, 1990; 357.
5. Shpiro ES, Minachev KM. *Catalyst Surface: Physical Methods of Studying*. CRC Press: Boca Raton, FL, 1990.
6. Grünert W. In *Spectroscopy of Transition Metal Ions on Surfaces*, Weckhuysen BM, Van Der Voort P, Catana G (eds). Leuven University Press: Leuven, 2000; 269.
7. González-Eliphe AR, Yubero F. In *Handbook of Surfaces and Interfaces of Materials*, Nalwa HS (ed), vol. 2. Academic Press: San Diego, 2001; 147.
8. Cimino A, de Angelis BA. *J. Catal.* 1975; **35**: 11.
9. Haber J, Marczewski W, Stoch J, Ungier L. *Ber. Bunsenges. Phys. Chem.* 1975; **79**: 970.
10. Zingg DS, Makovsky LE, Tischer RE, Brown FR, Hercules DM. *J. Phys. Chem.* 1980; **84**: 2398.
11. Yamada M, Yasumaru J, Houalla M, Hercules DM. *J. Phys. Chem.* 1991; **95**: 7037.
12. Quincy RB, Houalla M, Proctor A, Hercules DM. *J. Phys. Chem.* 1990; **94**: 1520.
13. Grünert W, Stakheev AY, Feldhaus R, Anders K, Shpiro ES, Minachev KM. *J. Phys. Chem.* 1991; **95**: 1323.
14. Taglauer E, Knözinger H. *Phys. Status Solidi B* 1995; **192**: 465.
15. Salvati Jr L, Makovsky LE, Stencel JM, Brown FR, Hercules DM. *J. Phys. Chem.* 1981; **85**: 3700.
16. Eberhardt MA, Houalla M, Hercules DM. *Surf. Interface Anal.* 1993; **20**: 766.
17. Fiedor JN, Proctor A, Houalla M, Sherwood PMA, Mulcahy FM, Hercules DM. *J. Phys. Chem.* 1992; **96**: 10967.
18. Vaidyanathan N, Houalla M, Hercules DM. *Catal. Lett.* 1997; **43**: 209.
19. Vaidyanathan N, Houalla M, Hercules DM. *Surf. Interface Anal.* 1998; **26**: 415.
20. Sazo V, Gonzalez L, Goldwasser J, Houalla M, Hercules DM. *Surf. Interface Anal.* 1995; **23F**: 367.
21. Fiedor JN, Houalla M, Proctor A, Hercules DM. *Surf. Interface Anal.* 1995; **23**: 234.
22. Eberhardt MA, Proctor A, Houalla M, Hercules DM. *J. Catal.* 1996; **160**: 27.
23. Meunier G, Mocaer B, Kasztelan S, LeCoustumer LR, Grimblot J, Bonelle JP. *Appl. Catal.* 1986; **21**: 329.
24. Houalla M, Kibby CL, Eddy EL, Petrakis L, Hercules DM. In *Proc. 8th Int. Congr. on Catalysis*, VCH Weinheim: Berlin, 1984; 147.
25. Grünert W, Stakheev AY, Mörke W, Feldhaus R, Anders K, Shpiro ES, Minachev KM. *J. Catal.* 1992; **135**: 269.
26. Liu HC, Weller SW. *J. Catal.* 1980; **66**: 65.
27. Briand LE, Tkachenko OP, Guraya M, Wachs IE, Grünert W. *J. Phys. Chem. B* submitted.
28. Hu H, Wachs IE, Bare SR. *J. Phys. Chem.* 1995; **99**: 10897.
29. Scofield JH. *J. Electron Spectrosc. Relat. Phenom.* 1976; **8**: 129.
30. Shirley DA. *Phys. Rev. B* 1972; **5**: 4709.
31. Goldwasser J, Fang SM, Houalla M, Hall WK. *J. Catal.* 1989; **115**: 34.
32. Aigler JM, Kazansky VB, Houalla M, Proctor A, Hercules DM. *J. Phys. Chem.* 1995; **99**: 11489.